Controlled growth of epitaxial BiFeO3 films using self-assembled BiFeO3-CoFe2O4 multiferroic heterostructures as a template

Yanxi Li, Yaodong Yang, Jianjun Yao, Ravindranath Viswan, Zhiguang Wang, Jiefang Li, and D. Viehland

Citation: Applied Physics Letters **101**, 022905 (2012); doi: 10.1063/1.4734508
View online: http://dx.doi.org/10.1063/1.4734508
View Table of Contents: http://scitation.aip.org/content/aip/journal/apl/101/2?ver=pdfcov
Published by the AIP Publishing

Controlled growth of epitaxial $BiFeO_3$ films using self-assembled $BiFeO_3$-$CoFe_2O_4$ multiferroic heterostructures as a template

Yanxi Li,[1,a)] Yaodong Yang,[2] Jianjun Yao,[1] Ravindranath Viswan,[1] Zhiguang Wang,[1] Jiefang Li,[1] and D. Viehland[1]
[1]*Department of Materials Science and Engineering, Virginia Tech, Blacksburg, Virginia 24061, USA*
[2]*Multi-Disciplinary Materials Research Center, Frontier Institute of Science and Technology, Xi'an Jiaotong University, Xi'an 710054, China*

(Received 10 May 2012; accepted 24 June 2012; published online 11 July 2012)

The growth mechanism of a $BiFeO_3$ layer deposited on self assembled (0.65) $BiFeO_3$-(0.35) $CoFe_2O_4$ (BFO-CFO) composite thin films was studied. Epitaxial and self-assembled BFO-CFO thin films were deposited on $SrTiO_3$ (111) substrates by pulsed laser deposition and were subsequently used as a seed layer for the deposition of an additional BFO layer. x-ray line scans showed the heterostructures were highly epitaxial. Cross-sectional scanning electron microscopy and focused ion beam images revealed the top BFO layer grew preferentially from BFO nanopillars in the BFO-CFO thin films, thus, demonstrating controlled growth. The multiferroic properties of this new nanostructure were then studied. © *2012 American Institute of Physics*. [http://dx.doi.org/10.1063/1.4734508]

Multiferroics, which are materials that have two or more of the so-called ferroic order parameters, have attracted a great deal of interest due to their potential in numerous applications such as switches, sensors, actuators, or new types of electronic memory devices.[1–5] The term multiferroic was first used by Schmid,[6] which initially only referred to single-phase materials but was later expanded to include any material that had two or more types of long-range spontaneous orderings. Most single-phase multiferroic materials have coexisting order parameters only at low temperatures: such limitations persisted for many years, until the emergence of composites.

The recent re-emergence of interest in multiferroics has been driven partially by the development of thin film growth techniques, which enable deposition under non-equilibrium conditions and epitaxial engineering.[7–9] Thin films have provided an opportunity to create and stabilize a number of new multiferroics. Multiferroic thin films have been deposited using a wide variety of growth methods such as pulsed laser deposition (PLD),[10–12] chemical vapor deposition (CVD),[13] molecular beam epitaxy (MBE),[14] sputtering,[15] spin coating,[16] and sol–gel processes.[17]

Compared with single-phase multiferroic thin films, two-phase nanocomposite ones have advantages with regards to compositional flexibility, phase distribution, and dimensional inter-connectivity and morphology.[18–24] Several different types of two-phase multiferroic nanocomposite epitaxial thin films have been reported, including nanoparticles with a (0–3) phase connectivity in a matrix,[25,26] epitaxial heterostructures of individual layers with a (2–2) connectivity,[27,28] and nanorods of one phase embedded in a matrix of the other with a (1–3) connectivity.[29–32] Amongst these, the (1-3) structures have attracted the great interest by researchers after it was first report by Zheng[9] for self-assembled composite epitaxial thin films consisting of $CoFe_2O_4$ nanopillars embedded in a $BaTiO_3$ matrix. Since then, several other systems such as $BiFeO_3$-$CoFe_2O_4$ (BFO-CFO) have been explored by numerous researchers. By depositing on differently oriented substrates, self-assembled epitaxial BFO-CFO composite thin films were found to have different multiferroic properties and completely distinct types of nanostructures. For example, on (001) $SrTiO_3$ (STO), CFO triangular nanopillars formed embedded in a BFO matrix; on (111) STO, BFO pyramidal nanopillars formed in a CFO matrix; and on (110) STO, the films formed as a maze pattern in which neither phase could be identified as the matrix or pillars. The phase which spreads as the matrix, versus the one which is spatially confined to become the nanopillars, depends on the wetting conditions between film and substrate.[33]

Based on these prior investigations of multiferroic nanostructures, one could ask the question if such nanostructures could be used as template to control grain growth of a second layer grown on top of the nanostructure. Pre-deposited metal particles have previously been used to as seeds to affect the growth mechanism of secondary layers.[34,35] Utilizing nanopillars inside self-assembled (1-3) nanostructures would be a unique means to control grain growth and subsequent related properties. Here, we have utilized self-assembled BFO nanopillars in a BFO-CFO two phase layer on (111) STO as a seed layer on which to deposit a secondary top $BiFeO_3$ layer by PLD. The growth mechanism of this secondary BFO layer has been investigated, and its multiferroic properties studied.

Two phase $0.65BiFeO_3$-$0.35CoFe_2O_4$ epitaxial thin films were first deposited by PLD on (111) oriented STO substrates. These self-assembled layers were then used as templates on which to deposit a secondary $BiFeO_3$ layer. The layers were deposited at 700 °C under a 90 mTorr oxygen partial pressure. The films were deposited using a Lambda 305i KrF laser with a wavelength of 248 nm, focused to a spot size of 2 mm^2, and incident on the surface of a target at an energy density of 3 J/cm^2. The distance between the substrate and target was 6 cm, and the base

[a)]Electronic mail: yanxili@vt.edu.

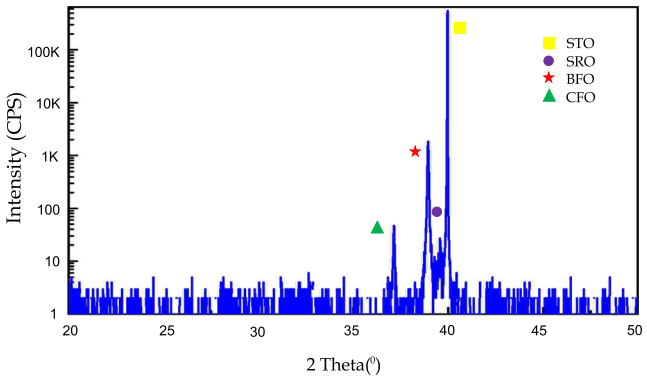

FIG. 1. X-ray diffraction line scan for two-layer BFO/BFO-CFO (111) oriented thin film.

vacuum of the chamber was 10^{-5} Torr. The crystal structures of the films were determined using a Philips X'pert high resolution x-ray diffractometer (XRD) equipped with a two bounce hybrid monochromator, and an open three-circle Eulerian cradle. The surface topology of the BFO-CFO thin films was studied by atomic force microscopy or AFM (Veeco 3100, Plainview, NY). Scanning electron microscopy or SEM images were obtained using a LEO 1550 high-performance Schottky field-emission SEM (Zeiss, Peabody, MA). A FEI Titan 300 high resolution transmission electron microscopy (HR-TEM) was used to obtain lattice images (FEI Company, Hillsboro, OR). Ferroelectric P-E hysteresis loops were measured by a modified Sawyer-Tower circuit. Magnetic hysteresis loops were measured using a vibrating sample magnetometer (VSM 7304, Lake Shore Cryotronics, Westerville, OH).

First, we investigated the structure of the BFO/BFO-CFO heterostructures by XRD as shown in Fig. 1. Single crystal peaks for (222) CFO, (111) BFO, (111) SRO, and (111) STO are clearly identified, which confirmed good epitaxy and phase purity. Figure 2(a) shows an AFM image of the surface topography. A uniform triangular BFO grain array was obvious on the surface. Top- and cross-sectional SEM images for a BFO/BFO-CFO film are shown in Figs. 2(b) and 2(c), respectively. One can see the same triangular-shaped BFO grain morphology similar to that in the AFM image, which was different than the topography of BFO-CFO template layer. For the self-assembled BFO-CFO layer, the BFO would be nanopillars embedded in a CFO matrix, which formed triangular shaped nanopillars whose apexes were distributed about the surface morphology. Different from that, the subsequently deposited BFO layer had no surrounded matrix to restrict its growth. Thus, it extended out along the lateral direction during deposition, which resulted in a uniform layer with a larger grain size on the surface. From the cross-section in Fig. 2(c), one can distinguish the STO substrate, a $SrRuO_3$ electrode layer, the BFO-CFO template layer, and the single phase BFO layer, from bottom to top, respectively. The thickness of the bottom BFO-CFO template layer was about 700 nm, with a growth rate of roughly 10 nm per minute. The thickness of top BFO layer was about 1400 nm, with a growth rate of roughly 15 nm per minute. In this figure, one can see that in the BFO-CFO seed layer, the BFO phase formed as nanopillars defined by (100) facets embedded in a CFO matrix, as previously reported.[33]

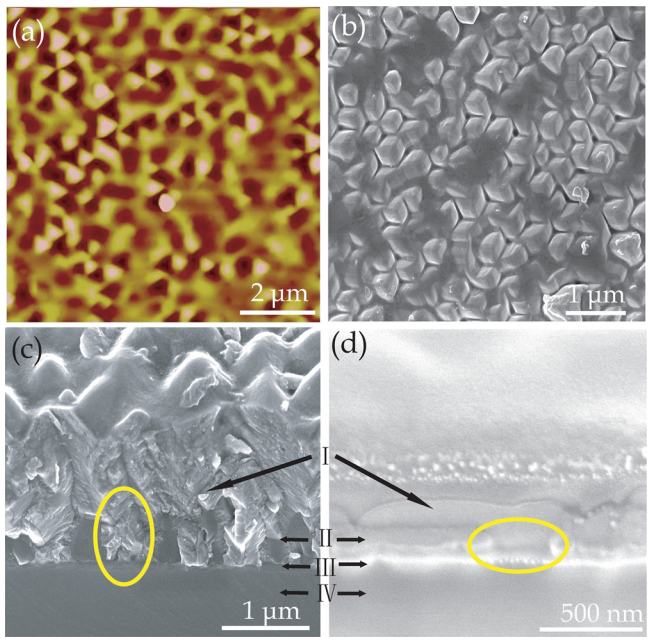

FIG. 2. (a) AFM image for two-layer BFO/BFO-CFO (111) oriented thin film; (b) scanning electron microscopy (SEM) images of surface top view; (c) 45° cross-section view of one BFO/BFO-CFO film; (d) cross-section area after cutting by focus ion beam (FIB) of another BFO/BFO-CFO film. Marked regions indicate BFO nanopillars which act as seeds in the bottom layer. Area I: BFO top layer. Area II: BFO-CFO template layer. Area III: $SrRuO_3$ electrode layer. Area IV: STO substrate.

The secondary BFO layer deposited on the BFO-CFO template then tended to preferentially grow from the BFO regions in this BFO-CFO layer. Clearly, the BFO nanopillars in the BFO-CFO layer act as seeds for the growth of the secondary top BFO layer.

It is well known that epitaxial thin film growth modes depend on several parameters, such as substrate and layer (layer and layer) misfits, misorientation of substrate, growth temperature, and atmosphere. Among these, the first two parameters are most important to determine the mode of nucleation and growth.[36] There are three classical growth modes: Volmer-Weber (VW), Frank-van der Merwe (FM), and Stranski-Krastonov (SK). Among these, VW growth occurs when adatom-adatom interactions are stronger than those of the adatom with the surface, leading to the formation of 3D adatom islands. In FM growth, adatoms preferentially attach to surface sites and result in atomically smooth 2D layers, whereas SK growth is an intermediate process consisting of both 2D layer and 3D island growth. From the cross-sectional SEM image of Fig. 2(c), we can see that the growth of top BFO layer on the BFO-CFO template follows a VW mode, as 3D BFO adatom islands grow preferentially on top of the BFO regions of the BFO-CFO template, which subsequently merge together during continued growth. By this type of 3D growth mechanism, it is reasonable to expect that templated layers could be used to control the grain size of the secondary top BFO layer. To confirm this possibility, a top BFO layer was deposited for a shorter time interval on top of BFO-CFO template. Cutting by focused ion beam (FIB), cross-sectional samples were obtained to study the morphology. In Fig. 2(d), the BFO grains in the top layer can be seen to grow from the BFO nanopillars in the BFO-CFO

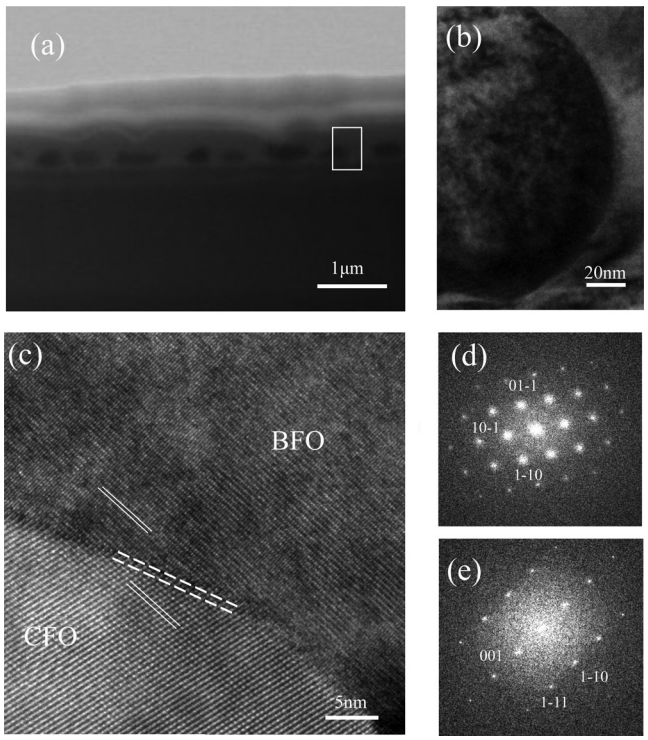

FIG. 3. (a) SEM image of cross-section area of lift-up slice from BFO/BFO-CFO thin film; (b) high resolution transmission electron microscopy (HR-TEM) image taken from a selected area of the SEM image given in (a); (c) lattice image of a higher resolution demonstrating a buffer zone between BFO and CFO phases; (d) and (e) power spectrum taken from CFO and BFO area from (c), respectively.

template and extend out along the lateral direction until adjacent grains begin to be connected. This demonstrates that the grain size of the secondary BFO layer can be controlled by templates by adjusting deposition time.

Figure 3(a) is the SEM image of the slice from BFO/BFO-CFO thin films by FIB lift up. Before ion-beam etching for reducing its thickness, which was used for latter TEM measurement, we could observe the same nanostructure like Fig. 2(d) from its cross-section view. High resolution TEM images in Fig. 3(b) is taken from the boxed-off area in this SEM image, demonstrating clear CFO and BFO phases indicated by the contrast at a lower magnification in the BFO-CFO bottom layer. As shown in Fig. 3(c), another HR-TEM image was then taken at a higher magnification from an interface area involving both BFO-CFO bottom layer and BFO top layer. Coherent lattice could be seen in the BFO region, which indicates smooth growth from bottom layer BFO nanopillar to top layer BFO without any defects existing. For the interface between CFO phase and BFO phase, no matter in top layer or bottom layer, we could observe the two regions separated by a buffer zone, which is less than 1 nm thick, as marked in the figure. The CFO phase region, which is viewed from [111] direction, is identified with an interplanar spacing a little bit larger than that of BFO phase region, which is viewed from its [110] direction. It could be found that the lattice orientation of these two phases are not exact the same, indicated by small angle between these lattice planes, partially elastically relaxed by the buffer zone. Such small incoherence is caused by the lattice mismatch and some defects and dislocations existing in the two phases interface. The power spectrums from the Fourier transform of both the CFO and BFO phase regions of the lattice image are shown in Figs. 3(d) and 3(e), respectively. Each of them contained a single set of reflections, revealing that they are single-phase CFO and BFO.

Next, the P-E loops for BFO/BFO-CFO heterostructures on (111) STO were measured at room temperature, as shown in Fig. 4(a). The saturation polarization was 70 μC/cm^2 with a remnant polarization of 43 μC/cm^2, and the coercive field was 23 kV/mm. One can see that although the P-E loop saturated, it was slightly asymmetric. This may be because of an internal bias field caused by defects from the interphase interfaces. Compared with the P-E loops of the BFO-CFO template, which had saturation polarization of 53 μC/cm^2, a remnant polarization of 34 μC/cm^2, and a coercive field of 20 kV/mm, we found that the ferroelectric properties had been improved. Figure 4(b) shows the longitudinal piezoelectric d_{33} coefficient measured by piezoforce microscopy (PFM). The value of d_{33} was about 25 pm/V. There was also some enhancement compared with the BFO-CFO template, with a d_{33} coefficient of 21 pm/V. Both the P-E loop and d_{33} measurements indicate that the BFO/BFO-CFO heterostructures had better ferroelectric properties. That is because after growing a top $BiFeO_3$ layer on the BFO-CFO two phase template, we switched the original (1-3) phase connectivity to a quasi-(0-3) connectivity, which changed the composite interconnectivity. Such BFO top layers, which had higher resistivity than the BFO-CFO template layer: limited by that of CFO, should be more capable of holding charge and thus enabling measurement of the polarization. The low resistivity ferromagnetic CFO lowered the net resistivity of the original BFO-CFO composite template layer, and accordingly resulted in dielectric leakage.

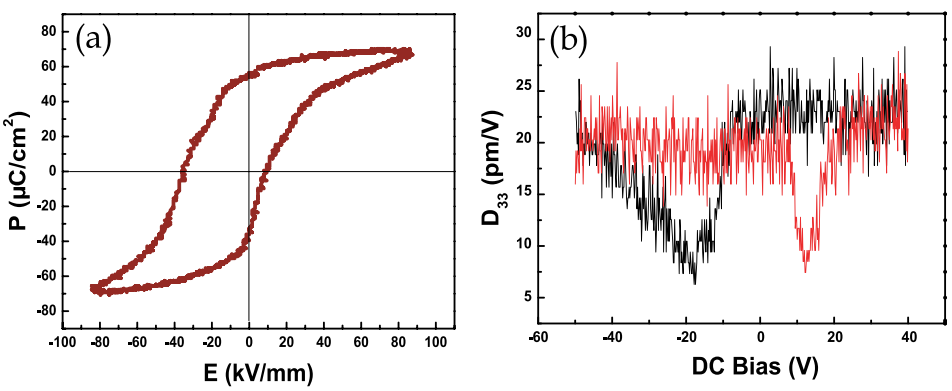

FIG. 4. (a) P-E hysteresis loops and (b) longitudinal piezoelectric d_{33} coefficient as a function of dc electric bias for (111) oriented BFO/BFO-CFO nanocomposite thin films.

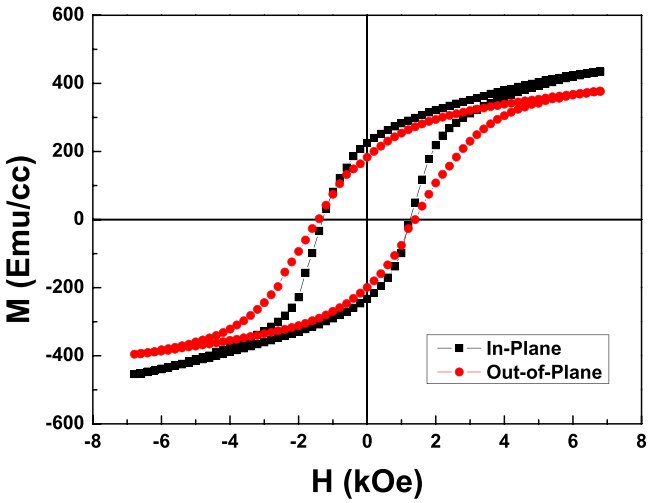

FIG. 5. Magnetization or M-H hysteresis loops in both in-plane and out-of-plane directions for (111) oriented BFO/BFO-CFO nanocomposite thin films. The magnetization was normalized to the volume fraction of the CFO phase.

Furthermore, with decreasing CFO ration and increasing BFO, the ferroelectric properties should improve.

Finally, the ferromagnetic properties of the BFO/BFO-CFO heterostructure were measured by VSM at room temperature, as shown in Fig. 5. The magnetization values were normalized to the volume fraction of the CFO phase in the BFO/BFO-CFO heterostructure. The shapes of both the in-plane and out-of-plane M-H hysteresis loops were found to be similar to that previously reported for self-assembled BFO-CFO and single phase CFO films,[37–40] with similar values of the coercive field H_C. Note that CFO forms a matrix phase in the BFO-CFO template layer on (111) STO. Thus, the CFO phase in the template layer is dimensionally interconnected along the in-plane direction. In this case, the spin state is more stable in the in-plane direction than along the out-of-plane one: thus, the remanent magnetization (M_R) along the in-plane direction was a little higher than that out-of-plane. It has been shown that epitaxial CFO films deposited on STO are under a compression in the in-plane direction. Since CFO has a significant negative magnetostriction, the magnetoelastic energy will tend to dominate, favoring the in-plane direction to be the easy axis.[37–40] However, the presence of a small anisotropy between the in-plane and out-of-plane directions is likely due to a small residual strain in the layers. Interestingly, the top BFO layer did not alter the strain state of the BFO-CFO template, and had negligible effect on its magnetic properties.

In summary, we have fabricated BFO/BFO-CFO heterostructures by pulsed laser deposition. The growth mechanism and multiferroic properties of these new heterostructures were investigated. It was found that the top BFO layer preferentially grew from the BFO nanopillars inside the BFO-CFO layer which acted as a template. The grain size of the top BFO layer could thus be controlled. The new heterostructures had better ferroelectric properties to that of BFO-CFO template on STO. In addition, good ferromagnetic properties similar to BFO-CFO were found: the top BFO layer did not alter the strain state of the BFO-CFO template, and thus had negligible effect on the magnetic properties.

We would like to gratefully acknowledge financial support from the U.S. Department of Energy under Contract No. DE-AC02-98CH10886 and the Office of the Air-Force Office of Scientific Research under Grant No. FA9550-09-1-0552. We also thank Zhipeng Tian for FIB and NCFL at VT for SEM work and other useful discussion.

[1]C. W. Nan, Phys. Rev. B **50**, 6082 (1994).
[2]J. Zhai, Z. Xing, S. Dong, J. Li, and D. Viehland, J. Am. Ceram. Soc. **91**, 351 (2008).
[3]S. X. Dong, J. R. Cheng, J. F. Li, and D. Viehland, Appl. Phys. Lett. **83**, 4812 (2003).
[4]S. X. Dong, J. F. Li, and D. Viehland, IEEE Trans. Ultrason. Ferroelectr. Freq. Control **50**, 1253 (2003).
[5]C. W. Nan, M. I. Bichurin, S. X. Dong, D. Viehland, and G. Srinivasan, J. Appl. Phys. **103**, 031101 (2008).
[6]H. Schmid, Ferroelectrics **162**, 317 (1994).
[7]D. G. Schlom, J. H. Haeni, J. Lettieri, C. D. Theis, W. Tian, J. C. Jiang, and X. Q. Pan, Mater. Sci. Eng., B **87**, 282 (2001).
[8]J. Wang, J. B. Neaton, H. Zheng, V. Nagarajan, S. B. Ogale, B. Liu, D. Viehland, V. Vaithyanathan, D. G. Schlom, U. V. Waghmare, N. A. Spaldin, K. M. Rabe, M. Wuttig, and R. Ramesh, Science **299**, 1719 (2003).
[9]H. Zheng, J. Wang, S. E. Lofland, Z. Ma, L. Mohaddes-Ardabili, T. Zhao, L. Salamanca-Riba, S. R. Shinde, S. B. Ogale, F. Bai, D. Viehland, Y. Jia, D. G. Schlom, M. Wuttig, A. Roytburd, and R. Ramesh, Science **303**, 661 (2004).
[10]Y. D. Yang, J. J. Yao, J. F. Li, J. Das, and D. Viehland, Thin Solid Films **518**, 5806 (2010).
[11]Y. D. Yang, J. J. Yao, J. F. Li, and D. Viehland, Mater. Lett. **65**, 1207 (2011).
[12]Z. G. Wang, Y. D. Yang, R. Viswan, J. F. Li, and D. Viehland, Appl. Phys. Lett. **99**, 043110 (2011).
[13]D. Kim, D. Klingensmith, D. Dalton, V. Olariu, F. Gnadinger, M. Rahman, A. Mahmud, and T. S. Kalkur, Integr. Ferroelectr. **68**, 75 (2004).
[14]Y. Chye, T. Liu, D. Li, K. Lee, D. Lederman, and T. H. Myers, Appl. Phys. Lett. **88**, 132903 (2006).
[15]D. C. Yoo, J. Y. Lee, I. S. Kim, and Y. T. Kim, Thin Solid Films **416**, 62 (2002).
[16]K. Suzuki, J. W. Cochrane, J. M. Cadogan, X. Y. Xiong, and K. Hono, J. Appl. Phys. **91**, 8417 (2002).
[17]K. T. Kim and C. I. Kim, J. Eur. Ceram. Soc. **24**, 2613 (2004).
[18]L. Yan, Y. D. Yang, Z. G. Wang, Z. P. Xing, J. F. Li, and D. Viehland, J. Mater. Sci. **44**, 5080 (2009).
[19]J. Ma, J. M. Hu, Z. Li, and C. W. Nan, Adv. Mater. **23**, 1062 (2011).
[20]I. Vrejoiu, M. Alexe, D. Hesse, and U. Gosele, Adv. Funct. Mater. **18**, 3892 (2008).
[21]A. Morelli, F. Johann, N. Schammelt, and I. Vrejoiu, Nanotechnology **22**, 265303 (2011).
[22]L. Yan, X. Zhao, J. F. Li, and D. Viehland, Appl. Phys. Lett. **94**, 192903 (2009).
[23]J. X. Zhang, B. Xiang, Q. He, J. Seidel, R. J. Zeches, P. Yu, S. Y. Yang, C. H. Wang, Y. H. Chu, L. W. Martin, A. M. Minor, and R. Ramesh, Nat. Nanotechnol. **6**, 97 (2011).
[24]S. A. Harrington, J. Y. Zhai, S. Denev, V. Gopalan, H. Y. Wang, Z. X. Bi, S. A. T. Redfern, S. H. Baek, C. W. Bark, C. B. Eom, Q. X. Jia, M. E. Vickers, and J. L. MacManus-Driscoll, Nat. Nanotechnol. **6**, 491 (2011).
[25]J. G. Wan, X. W. Wang, Y. J. Wu, M. Zeng, Y. Wang, H. Jiang, W. Q. Zhou, G. H. Wang, and J. M. Liu, Appl. Phys. Lett. **86**, 122501 (2005).
[26]H. Ryu, P. Murugavel, J. H. Lee, S. C. Chae, T. W. Noh, Y. S. Oh, H. J. Kim, K. H. Kim, J. H. Jang, M. Kim, C. Bae, and J. G. Park, Appl. Phys. Lett. **89**, 102907 (2006).
[27]J. P. Zhou, H. C. He, Z. Shi, and C. W. Nan, Appl. Phys. Lett. **88**, 013111 (2006).
[28]H. C. He, J. P. Zhou, J. Wang, and C. W. Nan, Appl. Phys. Lett. **89**, 052904 (2006).
[29]J. Slutsker, I. Levin, J. H. Li, A. Artemev and A. L. Roytburd, Phys. Rev. B **73**, 18 (2006).
[30]I. Levin, J. H. Li, J. Slutsker, and A. L. Roytburd, Adv. Mater. **18**, 2044 (2006).
[31]Q. Zhan, R. Yu, S. P. Crane, H. Zheng, C. Kisielowski, and R. Ramesh, Appl. Phys. Lett. **89**, 172902 (2006).
[32]H. Zheng, J. Wang, L. Mohaddes-Ardabili, M. Wuttig, L. Salamanca-Riba, D. G. Schlom, and R. Ramesh, Appl. Phys. Lett. **85**, 2035 (2004).

[33]H. Zheng, F. Straub, Q. Zhan, P. L. Yang, W. K. Hsieh, F. Zavaliche, Y. H. Chu, U. Dahmen, and R. Ramesh, Adv. Mater. **18**, 2747 (2006).
[34]X. N. Sun, M. P. Felicissimo, P. Rudolf, and F. Silly, Nanotechnology **19**, 495307 (2008).
[35]Y. D. Yang, J. J. Yao, Y. U. Wang, J. F. Li, J. Das, and D. Viehland, ACS Nano **3**, 3045 (2009).
[36]R. Ramesh and N. A. Spaldin, Nat. Mater. **6**, 21 (2007).
[37]R. Valenzuela, *Magnetic Ceramics* (Cambridge University Press, Cambridge, 1994).
[38]P. C. Dorsey, P. Lubitz, D. B. Chrisey, and J. S. Horwitz, J. Appl. Phys. **79**, 6338 (1996).
[39]Y. C. Wang, J. Ding, J. B. Yi, B. H. Liu, T. Yu, and Z. X. Shen, Appl. Phys. Lett. **84**, 2596 (2004).
[40]Y. Suzuki, Annu. Rev. Mater. Res. **31**, 265 (2001).